Dissociative recombination in low-energy e-H_2^+ collisions

A. Giusti-Suzor
Laboratoire de Photophysique Molèculaire, Université de Paris-Sud, F-91405 Orsay, France

J. N. Bardsley and C. Derkits
Physics Department, University of Pittsburgh, Pittsburgh, Pennsylvania 15260
(Received 22 September 1982)

The theory of configuration interaction in molecules is extended to permit the simultaneous treatment of doubly excited electronic states and vibrationally excited Rydberg states which can decay by autoionization and predissociation. The method is applied to dissociative recombination and compared with the corresponding multichannel quantum-defect theory. Calculations using both techniques are reported for collisions of electrons of energy below 0.5 eV with H_2^+ ions in the lowest three vibrational states. The Rydberg states lead to narrow structures in the cross sections, mostly in the form of dips. The cross section and recombination rate for ground-state ions are anomalously low, being smaller than those for $v=1$ and 2 by a factor of ~ 6.

I. INTRODUCTION

Although dissociative recombination has been studied for many years,[1,2] both experimentally and theoretically, there has not yet been a definitive comparison of theory and experiment. On the experimental side, it is very difficult to observe the recombination of ions in specific vibrational states, except perhaps by the trapped ion method,[3,4] which has been applied only to a small number of ions and in which the determination of absolute cross sections is difficult. In view of the significant difference in the measured recombination rates[2] for some molecules, such as NO^+, it would be valuable to have a simple reference system for which the recombination rate is well established. In calculations, the major problems arise in the determination of the energy and lifetimes of the intermediate molecular states through which the recombination proceeds, and from uncertainty about the role of vibrationally excited Rydberg states in the recombination process.

Theoretically, the most suitable ion for this comparison is H_2^+, since several calculations of the relevant molecular parameters have been performed.[5–8] Although it is difficult to produce a plasma in which H_2^+ is the dominant ion, experiments have been performed using inclined beams,[9] the hollow electron-beam trap[10] and the merged-beam method.[11] The cross sections measured by the merged-beam technique at energies below 3 eV showed narrow structures, mostly dips, superimposed upon a monotonically decreasing background with an energy dependence close to $E^{-0.9}$.

In order to reduce the uncertainty with respect to the vibrational level of the H_2^+ ions, Auerbach *et al.*[11] added He atoms to their ion source. The states of H_2^+ with $v>2$ can then be removed by the fast reaction

$$H_2^+ + He \rightarrow HeH^+ + H \ .$$

In this paper we will assume that the three remaining levels ($v=0,1,2$) were populated in the ratios 1:2:2, respectively. However, these populations must be regarded only as rough estimates.

Dissociative recombination of H_2^+ can be considered, most simply, in terms of the formation and dissociation of a doubly excited state of the H_2 molecule

$$e + H_2^+ \rightarrow H_2^{**} \rightarrow H + H^* \ . \tag{1}$$

This process, often called direct dissociative recombination, can be described theoretically by resonant scattering theory.[12–15] The most important parameters are the potential curves and autoionization rates of the intermediate states H_2^{**}. The lowest of these states is the $1\sigma_u^2\ ^1\Sigma_g^+$ state, whose properties were discussed in a previous paper.[6]

If these doubly excited states are coupled with the e-H_2^+ scattering continuum they must also interact with the manifold of Rydberg states $1\sigma_g nlm$ converging to the ground electronic state of H_2^+. In particular, the excited vibrational levels of these Rydberg states may play a role in dissociative recombination. In 1968 it was suggested[14] that the indirect process

$$e + H_2^+(v_i) \rightarrow H_2(n \geq 8, v_i + 1) \rightarrow H_2^{**} \rightarrow H + H^* \tag{2}$$

may contribute to recombination. In this process the Rydberg state is formed through the coupling of electronic and vibrational motion (the inverse of vibrational autoionization) and decays by predissociation due to electronic configuration interaction with the doubly excited state H_2^{**}. It was anticipated that for diatomic molecules this indirect process cannot dominate the direct mechanism in the overall recombination rate, but that it could lead to narrow structures in the recombination cross section.

More recent analyses[16,17] have demonstrated that the higher vibrational levels of Rydberg states with smaller n can hinder the recombination process. These levels may be coupled strongly to the dissociation continuum, but their direct coupling to the electron scattering continuum is weak, because of the propensity rule $\Delta v=1$ that applies to vibrational autoionization. Thus their contribution to process (2) is small. Instead, the chain

$$e + H_2^+(v=0) \rightarrow H_2^{**} \rightarrow H_2(n, v \geq 2) \rightarrow H_2^{**} \rightarrow H_2^+ + e \tag{3}$$

may interfere destructively with reaction (1).

O'Malley[17] has suggested that these Rydberg levels should be regarded as resonances in the dissociation continuum (corresponding to $H + H^*$ scattering). This approach stresses the importance of predissociation of the Rydberg levels, and seems appropriate when the direct coupling between the Rydberg state and the electron scattering continuum is weak. However, the treatment of the autoionization of the Rydberg states by indirect coupling through the doubly excited state [as in reaction (3)] is not so clear in O'Malley's approach. It has already been demonstrated[16,18] that multichannel quantum-defect theory (MQDT) gives a unified treatment of the decay of Rydberg states by predissociation and autoionization, and can be used in the calculation of cross sections for dissociative recombination. In this paper we will show that a unified theory can also be derived by the method of configuration interaction.[13,14] We will discuss the relative merits of these theoretical approaches and will apply the theories to e-H_2^+ recombination.

In this application we will concentrate on the low-energy region, below 0.5 eV, in which there is the most uncertainty about the recombination cross section. In particular, we will estimate the recombination rate at low temperatures, which is of cosmological interest.

There has been relatively little work on vibrational excitation in low-energy electron-ion collisions.[19] The intermediate states that are active in dissociative recombination will also lead to resonant vibrational excitation. The cross sections for this process can be obtained straightforwardly by the MQDT or configuration-interaction method. In Sec. IV C the results for H_2 will be compared with the nonresonant contributions to the same process.

We will begin with a development of configuration interaction theory to include the effects of Rydberg states upon direct recombination. Although the approach is based upon the earlier work by Bardsley,[14] the notation will be changed slightly to facilitate the comparison with the work of Giusti[16] and Lee,[18] as detailed in the Appendix.

II. CONFIGURATION-INTERACTION THEORY

Let us suppose that the wave function representing the scattering of an electron by a molecular ion can be separated into three components representing the nonresonant electron scattering continua, the formation of a doubly excited electronic state, and the formation of vibrationally excited Rydberg states. Using Q to denote the coordinates of all of the electrons, we write

$$\Psi(q,R)=\sum_v \int dE' b_v(E')\psi_{vE'}(q,R)\chi_v(R) + \phi_d(q,R)\zeta_d(R) + \sum_{p,v} a_{pv}\psi_p(q,R)\chi_v(R) . \quad (4)$$

In the first term we have assumed that nonresonant vibrational excitation is not important and that the associated wave function can be written as the product of an electronic function $\psi_{vE'}(q,R)$ and the vibrational wave function of the molecular ion, $\chi_v(R)$. In most applications the dependence of $\psi_{vE}(q,R)$ upon v will arise solely because the energy available to the extra electron depends on v as well as the total energy E. Throughout the paper we will neglect molecular rotations, which are only important at very high gas temperatures. For the doubly excited configuration we assume that the electronic wave function $\phi_d(q,R)$ is known, along with the associated potential-energy curve $E_d(R)$, given by

$$E_d(R)=\langle \phi_d(q,R) \mid H_{\rm el}(q,R) \mid \phi_d(q,R)\rangle . \quad (5)$$

The nuclear function $\zeta_d(R)$ is to be determined by the theory.

In the final term in Eq. (3), the electronic wave functions for the Rydberg states $\psi_p(q,R)$ are also regarded as known; p is used as a collective index to indicate all of the quantum numbers of the Rydberg electron, in particular, its principal quantum number n, orbital angular momentum l, and its component about the nuclear axis λ. The energy of the Rydberg state will be denoted by E_{pv}.

Let us now examine the couplings, between the three terms of Eq. (4), induced by the total Hamiltonian $H(q,R)$ which can be written as the sum of the nuclear kinetic-energy operator and the electronic Hamiltonian

$$H(q,R)=T_R+H_{\rm el}(q,R) . \quad (6)$$

The doubly excited electronic state $\phi_d(q,R)$ is coupled by the electronic Hamiltonian to both the electronic scattering continua and the Rydberg manifold. Let us define

$$V_{\rm el}(E,R)=\langle \psi_{vE}(q,R) \mid H_{\rm el}(q,R) \mid \phi_d(q,R)\rangle \quad (7)$$

and

$$d_v=\langle \chi_v(R) \mid V_{\rm el}(E,R) \mid \zeta_d(R)\rangle . \quad (8)$$

Because of the strength of the Coulomb interaction between the electron and ion, the shape of the electronic wave functions for the high Rydberg states $\psi_p(q,R)$ and those representing scattering at low energies differ only in the asymptotic region. Thus we can usually neglect the energy dependence of $V_{\rm el}(E,R)$ and can write

$$\langle \psi_p(q,R) \mid H_{\rm el}(q,R) \mid \phi_d(q,R)\rangle=\rho_p V_{\rm el}(R) \quad (9)$$

in which ρ_p is determined by the density of states. If the effective principal quantum number of the Rydberg state is n^*, then

$$\rho_p \approx (n^*)^{-1.5} . \quad (10)$$

The Rydberg states and electron scattering continua are coupled through the nuclear kinetic-energy operator. Let us write

$$\langle \psi_p(q,R)\chi_{v'}(R) \mid T_R \mid \psi_{vE}(q,R)\chi_v(R)\rangle=\rho_p W_{v'v} . \quad (11a)$$

It is well known from the study of vibrational autoionization[20,21] that $W_{v'v}$ is large only when $v'=v+1$. For this case, using harmonic-oscillator wave functions for χ_v and $\chi_{v'}$, by making a Taylor-series expansion of $\mu(R)$, we find[21,22]

$$W_{v'v}=\left[\frac{v'}{2M\omega}\right]^{1/2}\frac{d\mu}{dR} , \quad (11b)$$

where ω is the vibrational frequency of the ionic core.

The wave function described in Eq. (4) can be used to

study a variety of processes. To describe the scattering of an electron by a molecular ion in a specific vibrational state v_i, we must ensure that the only incoming waves occur in the component of the first term with $v=v_i$ and that $\zeta_d(R)$ is purely outgoing. The dissociative recombination cross section can then be found from the asymptotic magnitude of $\zeta_d(R)$.

The unknown expansion coefficients a_p, $b_v(E')$, and $\zeta_d(R)$ are obtained by projections of the Schrödinger equation

$$[T_R+H_{\rm el}(q,R)-E]\Psi(q,R)=0 . \tag{12}$$

Premultiplying by $\psi_E^*(q,R)\chi_k^*(R)$ and integrating over all coordinates gives

$$(E'-E)b_{v'}(E')+\sum_{p,v}\rho_p W_{v'v}a_{pv}+d_{v'}=0 . \tag{13}$$

Imposing the boundary condition described above, we find

$$b_{v'}(E')=\delta_{v'v_i}\delta(E-E')+\left[\frac{1}{E-E'}+\pi i\delta(E-E')\right]\times\left[\sum_{p,v}\rho_p W_{v'v}a_{pv}+d_{v'}\right] . \tag{14}$$

The term $(E-E')^{-1}$ leads through principal part integrals to level shifts associated with autoionization. These shifts are negligible for the Rydberg states, and for the doubly excited state we will assume that they have been included in the potential energy $E_d(R)$.

The coefficients a_{pv} can now be obtained by premultiplying Eq. (12) by $\psi_p^*(q,R)\chi_v^*(R)$ and integrating again overall coordinates, which gives

$$(E-E_{pv'})a_{pv'}=\rho_p d_{v'}+\sum_v \rho_p W_{v'v}b_v(E) . \tag{15}$$

Finally, we premultiply Eq. (12) by $\phi_d(v,R)$ and integrate over the electronic coordinates to obtain a differential equation for $\zeta_d(R)$, namely,

$$\left[-\frac{\hbar^2}{2M}\frac{d^2}{dR^2}+E_d(R)-E\right]\zeta_d(R)=-V_E(R)\left[\chi_{v_i}(R)-i\pi\sum_v d_v\chi_v(R)+\sum_{p,v}\rho_p a_{pv}\left[\chi_v(R)-i\pi\sum_{v'}W_{vv'}\chi_{v'}(R)\right]\right] . \tag{16}$$

On the right-hand side of this equation, the first two terms describe the formation and decay of the doubly excited state through direct coupling to the electron scattering continuum, the third term expresses the predissociation of the Rydberg state, and the final term arises from indirect coupling involving the Rydberg states and the continuum.

Equation (16) can be solved in terms of the Green function

$$\left[-\frac{\hbar^2}{2M}\frac{d^2}{dR^2}+E_d(R)-E\right]G(R,R')=\delta(R-R') . \tag{17}$$

Multiplication by $\zeta_v^*(R)V_{\rm el}^*(R)$ and integration over R then leads to the coupled equations

$$d_v=-g_{vv_i}+i\pi\sum_{v'}\left[d_{v'}g_{vv'}-\sum_p\rho_p a_{pv}\left[g_{vv'}-i\pi\sum_{v''}g_{vv''}W_{v''v'}\right]\right] , \tag{18}$$

where

$$g_{vv'}=\int\int dR\,dR'\chi_v^*(R)V_{\rm el}^*(R)G(R,R')V_{\rm el}(R')\chi_{v'}(R') . \tag{19}$$

Although $G(R,R')$ and $g_{vv'}$ are functions of E, we will not indicate this dependence explicitly since they will always be evaluated at the experimental energy E.

The equations (14), (15), and (18) form a set of linear algebraic equations for the coefficients a_{pv}, b_v, and d_v that can be solved by standard numerical techniques, once the matrix elements $g_{vv'}$ have been evaluated.

To illustrate the solution, let us consider a single Rydberg state (pv) interacting with one electron scattering continuum $\psi_E(r,R)\chi_{v_i}(R)$. This could apply to electron collisions with ground-state ions at an energy below the threshold for vibrational excitation, if the Rydberg level is well isolated. The amplitude of the Rydberg state is then

$$a_{pv}=\frac{-\beta\rho_p(W_{vv_i}+g_{vv_i})}{E_{pv}-E+\rho_p^2 g_{vv}-\pi i\beta\rho_p^2(W_{vv_i}+g_{vv_i})^2} , \tag{20}$$

where

$$\beta=(1+i\pi g_{v_iv_i})^{-1} . \tag{21}$$

This expression shows that the Rydberg state can be formed in two ways, either directly through vibrational capture or indirectly via the doubly excited state. The Rydberg state leads to a Siegert resonance at the complex energy at which the denominator vanishes, i.e., at

$$E=E_{\rm res}=E_{pv}+\rho_p^2 g_{vv_i}-\pi i\beta\rho_p^2(W_{vv_i}+g_{vv_i})^2 . \tag{22}$$

Note that the matrix elements g_{vv_i} are complex. The second and third terms can be regarded as the complex energy shifts arising from predissociation and autoionization, respectively.

The Green function $G(R,R')$ can be computed most conveniently from two solutions of the corresponding homogeneous equation. We write

$$G(R,R')=\frac{1}{C}F_{1E}(R_<)F_{2E}(R_>) , \tag{23}$$

where $F_{1E}(R)$ and $F_{2E}(R)$ both satisfy

$$\left[-\frac{\hbar^2}{2M}\frac{d^2}{dR^2}+E_d(R)-E\right]F_{iE}(R)=0\ . \tag{24}$$

C is the Wronskian $[F_{1E}(R),F_{2E}(R)]$, and $R_<$ and $R_>$ are the lesser and greater of R and R'. The boundary conditions appropriate to $\zeta_d(R)$ will be satisfied if $F_{1E}(R)$ is regular at $R=0$ and if $F_{2E}(R)$ is purely outgoing as $R\to\infty$. This approach gives both the real and imaginary parts of the matrix elements $g_{vv'}$ without the calculation of any principal part integrals, which is necessary when using a spectral representation of the Green function. The link between the two approaches can be expressed in terms of the integrals

$$V_v(E)=\int\chi_v(R)V_{\rm el}(R)F_{1E}(R)dR \tag{25}$$

which can be assumed to be real. If we normalize $F_{1E}(R)$ and $F_{2E}(R)$ so that

$$\int F_{1E}(R)F_{1E'}(R)dR=\delta(E-E') \tag{26}$$

and

$$F_{2E}(R)=e^{iKR}\ \text{ as }\ R\to\infty \tag{27}$$

then

$$\mathrm{Re}g_{vv'}=\mathscr{P}\int dE'\frac{V_v(E')V_{v'}(E')}{E'-E} \tag{28}$$

and

$$\mathrm{Im}g_{vv'}=-\pi V_v(E)V_{v'}(E)\ . \tag{29}$$

Given the matrix elements $g_{vv'}$, the coefficients a_{pv}, $b_v(E')$, and d_v, and the nuclear wave function $\zeta_d(R)$, the cross section for dissociative recombination can be obtained by comparing the incident and outgoing fluxes of electrons. For electrons with energy ϵ,

$$\sigma_{\rm DR}(\epsilon)=\frac{\pi^2}{\epsilon}\frac{\omega}{2}\frac{\hbar K}{M}\lim_{R\to\infty}|\zeta_d(R)|^2 \tag{30}$$

in which ω is the ratio of the multiplicity of the doubly excited state to that of the initial electronic state of the ion, and $(\hbar K/M)$ is the relative velocity of the dissociation fragments. For our simple example of one Rydberg state and one electron scattering continuum, we find that as $R\to\infty$

$$\begin{aligned}\zeta_d(R)&=-\frac{1}{C}e^{iKR}\{V_{v_i}(1-\pi i d_{v_i})+\rho_p a_{pv}[V_v(E)-\pi i W_{vv_i}V_{v_i}(E)]\}\\&=\frac{\beta e^{iKR}}{C(E-E_{\rm res})}\{V_{v_i}(E)(E_{pv}-E)+\rho_p^2[V_{v_i}(E)g_{vv}-V_v(E)(W_{vv_i}+g_{vv_i})]\}\ .\end{aligned} \tag{31}$$

Because of Eq. (20), the contributions from the imaginary parts of g_{vv_i} and g_{vv} cancel, and $\zeta_d(R)$ vanishes at some energy close to E_{pv}. The cross section exhibits a Beutler-Fano profile, but the shape parameter q does not appear to have a simple interpretation. In particular, q is not directly proportional to W_{vv_i}, and q may be nonzero even if W_{vv_i} vanishes. Thus Rydberg states which are not directly coupled to the electron scattering continuum do not necessarily lead to window resonances.

The Rydberg states discussed above are examples of discrete levels embedded, through autoionization and predissociation, in two continua which are themselves strongly coupled. The application of configuration-interaction theory to this type of problem has been studied by Fano and Prats,[23] Nitzan,[24] and by Lefebvre and Beswick.[25] Their results can be recovered from ours if we neglect the real parts of the matrix elements g_{vv_i} which represent the dispersive parts of the second-order interaction with the dissociation continuum. Using Eqs. (22) and (27) we then obtain a resonance width

$$\Gamma_{pv}=2\pi\beta\rho_p^2(V_v^2+W_{vv_i}^2) \tag{32}$$

and a shift

$$\Delta_{pv}=-2\pi^2\beta\rho_p^2W_{vv_i}V_v(E)V_{v_i}(E)\ . \tag{33}$$

As noted previously,[24,25] the level shift is nonzero even when all principal part integrals are neglected.

The classic paper of Fano[13] addressed the problem of a doubly excited state of an atom embedded in a continuum of electron-ion scattering states. Nitzan[24] extended the model by considering radiative transitions between the doubly excited state and electron-ion scattering continuum and the ground state of the neutral atom, thus introducing a radiative continuum of photon-atom scattering states. The width of the doubly excited state is then composed of two parts, a radiative width Γ_R, and a nonradiative (autoionizing) component $\Gamma_{\rm NR}$. This system is clearly analogous to our Rydberg state coupled to an electron scattering continuum (autoionization) and an atom-atom scattering continuum (predissociation). Dissociative recombination involves a transition from one continuum to the other. The corresponding process in Nitzan's problem would be a transition from the radiative continuum to the electron scattering continuum, i.e., photoionization of the atomic ground state. Neglecting the dispersion terms, our $\sigma_{\rm DR}(\epsilon)$ is equivalent to the $\sigma_{\rm NR}$ of Nitzan, as given by Eq. (48) of his paper.[24] The Fano shape parameter is found to be

$$q=\frac{1-\pi^2V_{v_i}^2(E)}{\pi V_{v_i}(E)}\frac{W_{vv_i}V_v(E)}{V_v^2(E)+W_{vv_i}^2}\ . \tag{34}$$

This vanishes when either $W_{vv_i}=0$ or $V_v=0$, that is, when the direct coupling of the Rydberg state to the electron continuum or to the dissociation continuum is negligible.

In the applications described below we will show that, even when the principal part of the integrals in $g_{vv'}$ are not neglected, q is still small for most Rydberg states. This is due essentially to the weakness of the vibrational coupling, because of the slow variation of μ with R [see Eq. (11)]. Most of the resulting structures are very close to pure win-

dow resonances ($q=0$) and lead to a reduction in the recombination rate.

Application to a model problem. At an early state in this work we performed some calculations which illustrate well two very different interference patterns resulting from the presence of the Rydberg states. The calculations were performed with a potential curve

$$E_d(R)=E_u^+(R)-0.23 \tag{35}$$

in which $E_u^+(R)$ is the electronic energy of the $1\sigma_u$ excited state of H_2^+. This curve $E_d(R)$ crosses the ground-state potential for H_2^+. This curve $E_d(R)$ crosses the ground-state potential for H_2^+ near $2.8a_0$, which is well outside the Franck-Condon region for the ground vibrational state. The resonance width $\Gamma(R)$ was as given in Eq. (44) below. The matrix elements describing vibrational coupling were obtained with the use of Eq. (11b) with $d\mu/dR=0.1$ a.u.

In Fig. 1 we show the cross sections for recombination to ions with $v_i=0$ [Fig. 1(a)] and $v_i=1$ [Fig. 1(b)]. Contributions from Rydberg states with $v=v_i+1$ are included in the calculations. For $v_i=0$ the Rydberg states enhance the recombination cross section. This is because the direct recombination process is very weak, whereas the vibrational coupling is relatively strong. The formation of the Rydberg state increases the amplitude of the nuclear motion and thereby facilitates the formation of the doubly excited state which leads to dissociation. However, when the ion is initially in an excited vibrational level [Fig. 1(b)], the q value defined by Eq. (34) is small and the interference is mostly destructive.

The results shown in Fig. 1 are very similar to those arising from a three-channel MQDT calculation (see Sec. III). The shapes of the structures are almost identical, although there is a small difference in the positions of the structures due to the neglect of principal part integrals in the MQDT theory.

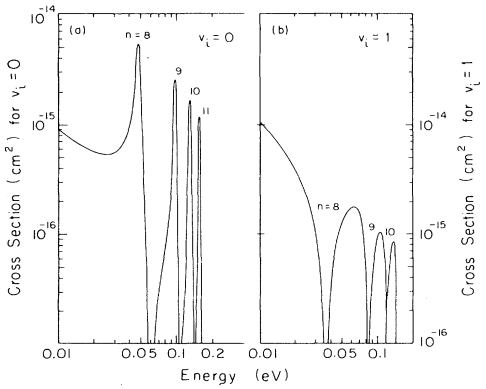

FIG. 1. Cross section for dissociative recombination in e-H_2^+ collisions computed by the CI method using the resonance potential curve in Eq. (35), for (a) ions with $v=0$ and (b) ions with $v=1$. Peaks in (a) arise from Rydberg states with $v=1$ and n as marked. Dips in (b) arise from Rydberg states with $v=2$. Each series should extend to $n=\infty$ at the vibrational excitation threshold (close to 0.27 eV).

III. MULTICHANNEL QUANTUM-DEFECT THEORY

Although the formalism described in Sec. II can be applied to problems involving an arbitrary number of Rydberg levels interacting with several electron scattering continua, it relies on the solution of a large set of algebraic equations and its implementation becomes difficult when many Rydberg levels are involved. If one wishes to see the effect of several manifolds of Rydberg states, then the use of quantum-defect theory is advantageous since each series, characterized by the quantum numbers $l\lambda v$, is treated as a single channel along with the adjacent continuum. The application of MQDT to dissociative recombination has been discussed by Lee[18] and by Giusti,[16] whose theory is based on the analysis of molecular Rydberg states by Jungen and his colleagues.[26,27] Since a detailed description of the method has been given elsewhere,[16] we will include here only a brief outline of the theory with some comments on the connections between the two approaches.

The basic concept of MQDT, allowing a unified treatment of bound states and continua, is the distinction between short- and long-range interactions. Configuration space is first divided into two regions. In the core region (Lee's reaction zone), all four particles interact strongly and the Born-Oppenheimer approximation is valid. In the external region, at least one interparticle distance is large and each departing particle experiences only a long-range local potential. The external zone thus allows for ionization or dissociation.

The MQDT does not attempt to provide an explicit representation of the wave function in the reaction zone, but only of the effect of the interactions within that region upon the solutions in the external zone. For the ionization channels, the core effects are mainly represented through the quantum defect μ, or phase shift $\pi\mu$, which is almost independent of energy on both sides of the threshold but may vary strongly with the nuclear separation R. In our diabatic approach, the dissociative channel wave function is written as the product of the electronic wave function $\phi_d(q,R)$ of Eq. (5) and the regular nuclear function $F_d(R)\equiv F_{1E}(R)$, defined in Eqs. (24) and (26).

Within the reaction zone the configuration mixing is governed by the electronic coupling $V_{el}(R)$ [see Eq. (9)] from which the vibronic matrix elements V_v are computed, as in Eq. (25). We will now recall briefly how these reaction zone parameters are used to describe the mixing of channels in the external zone.

A. Vibrational coupling between ionization channels

For large values of an electronic coordinate r, the external zone is subdivided into two regions. In region A, close to the core boundary r_0, the wave function for each ionization channel may still be expressed as a Born-Oppenheimer (BO) product

$$\Psi_v^A=\chi_v(R)\phi_{\text{core}}(r_c,R) \times\{f_l(\epsilon,r)\cos[\pi\mu(R)]-g_l(\epsilon,r)\sin[\pi\mu(R)]\}\ , \tag{36}$$

where $\phi_{\text{core}}(r_c,R)$ is the electronic wave function for the

ionic core; f_l and g_l are Coulomb wave functions, f_l being regular at the origin and g_l lagging in phase by $\pi/2$ in the asymptotic region. The vibrational wave function is approximated by the ionic eigenfunction χ_v, as in Sec. II.

In region B ($r \gg r_0$), the external electron is completely disconnected from the core and the coefficients of f_l and g_l are independent of R,

$$\Psi_v^B = \chi_v(R)\phi_{\text{core}}(r_c,R)[\alpha_v f_l(\epsilon,r) - \beta_v g_l(\epsilon,r)] \ . \tag{37}$$

To connect these two regions, we expand

$$\Psi_v^A = \sum_{v'} \chi_{v'}(R)\phi_{\text{core}}(r_c,R)[\mathscr{C}_{v'v} f_l(\epsilon,r) - \mathscr{S}_{v'v} g_l(\epsilon,r)] \ , \tag{38}$$

where the frame-transformation coefficients

$$\begin{aligned} \mathscr{C}_{v'v} &= \int \chi_{v'}(R)\cos[\pi\mu(R)]\chi_v(R)dR \ , \\ \mathscr{S}_{v'v} &= \int \chi_{v'}(R)\sin[\pi\mu(R)]\chi_v(R)dR \ , \end{aligned} \tag{39}$$

measure the mixing between ionization channels. The magnitude of the coupling depends clearly on the variations of the quantum defect with R, and transitions with $\Delta v = 1$ are favored.

These coefficients are closely related to the dimensionless matrix elements $W_{v'v}$, defined in Eq. (11) of Sec. II. If we write $\mu(R) = \mu(R_0) + (R - R_0)d\mu/dR$ and assume $v' = v + 1$ we find[22]

$$\begin{aligned} \mathscr{C}_{v'v} &= -\sin[\pi\mu(R_0)]W_{v'v} \\ \text{and} \qquad & \qquad (40) \\ \mathscr{S}_{v'v} &= \cos[\pi\mu(R_0)]W_{v'v} \ . \end{aligned}$$

B. Coupling between the ionization and dissociation channels

Let us now examine the coupling that arises from the reaction zone. The direct coupling between ionization channels, $V_{vv'}$, is taken to be zero, since the BO separation is assumed both in the reaction zone and external region A. Each ionization channel is coupled to the dissociation channel by a matrix element V_{vd} which is equivalent to the $V_v(E)$ defined in Eq. (25). From this coupling matrix we can define the short-range K matrix.[16] However, as in previous works,[16,18] we will approximate K by V, neglecting the dispersive part of the interaction (principal part integrals). This approximation is avoided in the configuration-interaction (CI) formalism by the Green-function method described in Sec. III.

To take account of the effect of this K matrix upon the external zone solutions, we introduce a set of eigenchannels Ψ_α as linear combinations of the ionization channels, as defined in zone A by Eq. (35) and of the dissociation channel

$$\begin{aligned} \Psi_\alpha = \sum_v U_{v\alpha}\chi_v(R)\phi_{\text{core}}(r_c,R)\{f_l(\epsilon,r)\cos[\pi\mu(R)+\eta_\alpha] - g_l(\epsilon,r)\sin[\pi\mu(R)+\eta_\alpha]\} \\ + U_{d\alpha}\phi_d(q,R)[F_d(R)\cos\eta_\alpha - G_d(R)\sin\eta_\alpha] \ . \end{aligned} \tag{41}$$

Here U is the unitary matrix which diagonalizes the K matrix, with eigenvalues $-\tan\eta_\alpha$; G_d is a second real solution of Eq. (24), lagging in phase by $\pi/2$ with respect to F_d. Thus the configuration mixing leads to an additional phase shift η_α in the asymptotic form of each channel wave function.

C. Boundary conditions and cross sections

The total wave function is expanded in the form

$$\Psi(q,R) = \sum_\alpha A_\alpha \Psi_\alpha(q,R) \ . \tag{42}$$

Imposition of the boundary conditions leads to a set of linear equations for the coefficients A_α. It is only at this stage that bound and continuum states are distinguished, as closed or open channels, respectively. The solutions A_α are then used to generate the S matrix from which cross sections can be calculated.[16]

IV. APPLICATION TO H_2^+

A. Recombination cross sections

The lowest doubly excited state of H_2 is the $^1\Sigma_g^+$ state which is dominated by the configuration $1\sigma_u^2$. The properties of that state were discussed in Ref. 6. The potential curve crosses that of H_2^+ near $2.65a_0$, at a point between the outer turning points of the ground and first excited states. The strength of the coupling with the electron scattering continuum increases wth increasing R, but is also sensitive to the energy of the continuum electron. There seems now to be good agreement concerning the potential curve and the autoionization rate. The major uncertainty that remains concerns the relative magnitude of the partial widths associated with coupling to the $s\sigma$ and $d\sigma$ partial waves. The scattering calculations indicate that the autoionization leads almost entirely to the emission of electrons with $l = 2$. On the other hand, analyses of the effect of the $1\sigma_u^2$ configurations upon the Rydberg states suggest that the coupling with the configurations $1s\sigma,ns\sigma$ is not negligible, although it is weaker than the coupling with states $1s\sigma nd\sigma$ at the value of n.

In most of the calculations described below the potential curve for the resonant state was assumed to be, in a.u.,

$$E_d(R) = \begin{cases} E_u^+(R) - 0.119 + 0.0417R - 0.008R^2, & R \le 2.4a_0 \\ 5.7936Re^{-1.49R} - R^{-1} - 0.5094, & 2.4a_0 \le R \le 3.5a_0 \\ -0.7145 + 0.0895(1 - e^{-0.5048(R-4.4)})^2, & R \ge 3.5a_0 \ . \end{cases} \tag{43}$$

The first segment is fitted to the algebraic variational calculation of Takagi and Nakamura[7] and incorporates the energy shift arising from the mixing with the electron scattering continuum. The second segment is deduced from the Rydberg-state deperturbation analysis of the work of Ref. 6, and the final segment is used to ensure dissociation to the limit $H(1s)+H(2s)$. $E_u^+(R)$ indicates the potential curve for the lowest $^2\Sigma_u$ state of H_2^+, which is the parent of this Feshbach resonance.

Although the strength of the coupling between the $1\sigma_u^2$ configuration and the electron scattering continuum varies significantly when the electron energy is varied by several eV, there is little change for energies between zero and 1 eV. Thus we use the coupling matrix elements $V_{el}(E,R)$ obtained by the Stieltjes method[6] with continuum electrons of zero energy. For $R \leq 4a_0$, we take (in a.u.)

$$\Gamma(R)=2\pi \mid V_{el}(R) \mid^2 = 0.0008R^3+0.0023R^2+0.0118R-0.0058 . \quad (44)$$

We have no information on $\Gamma(R)$ at larger values of R and so we assume it to be constant and equal to $\Gamma(4)$. This region has very little effect on the results presented below.

Finally, we need to characterize the Rydberg states. We have taken account only of the dominant $d\sigma$ manifold. In the Rydberg-state analysis, the quantum defect for this series was represented by

$$\mu_d(R)=0.055+0.048(R-2.5)+0.05(R-2.5)^2 . \quad (45)$$

This result is needed to determine the position of the unperturbed Rydberg levels E_{pv} and the vibronic coupling coefficients, $W_{v'v}$ from Eq. (11a), or $\mathscr{C}_{v'v}$ and $\mathscr{S}_{v'v}$ from Eq. (39). Although these were computed using numerically generated vibrational wave functions estimates of the values for $v'=v+1$ can be obtained using Eq. (11b).

In comparison to the model used in Sec. II, the potential curve given by Eq. (43) is significantly lower, and the vibrational coupling is much weaker. The resulting cross sections are shown in Fig. 2. This figure includes direct recombination cross sections, obtained by each method, and the full results of an MQDT calculation with 11 channels, including vibrational states 0—9 and the dissociation channel. Almost all of the Rydberg states lead to dips, and the origin of some of the more prominent dips is indicated on the diagram.

The direct recombination cross section drops significantly at each threshold for vibrational excitation. This is due to the extra competition from autoionization through the additional channel. The inclusion of the Rydberg states leads almost entirely to dips in the cross section which mask this discontinuity across vibrational excitation thresholds. One can regard these dips as precursors, in closed channels, of the additional autoionization that results as each vibrational channel opens. This effect is also seen in molecular photoionization spectra, where a new threshold is often masked by the autoionization peaks due to the Rydberg series converging to that threshold. The cross section for recombination to vibrationally excited ions is again larger than that for ground-state ions, although the enhancement is less pronounced than for the higher potential curve associated with Fig. 1.

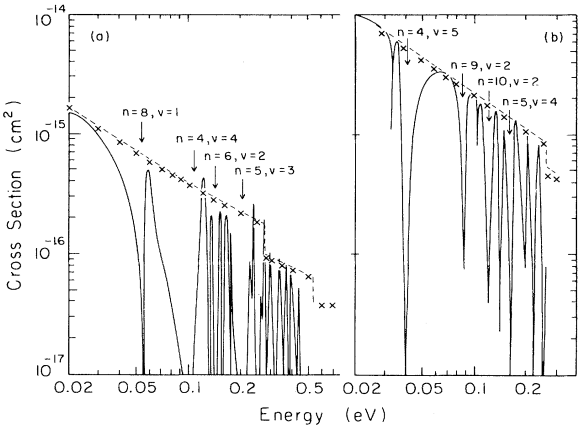

FIG. 2. Cross sections for dissociative recombination of electrons with H_2^+ ions in (a) the ground vibrational state and (b) the state $v=1$. Solid curve shows the results of an 11-channel MQDT calculation. Dips are due to Rydberg states of the $(nd\sigma,v)$ manifolds, with the values of n and v indicated for the most prominent dips. Dashed curve shows the result obtained with no closed channels and the crosses give the values obtained in the corresponding CI calculation.

The rapid oscillations in the calculated cross sections make comparison with experiment difficult, although our results do support the existence of narrow window resonances as observed by Auerbach *et al.*[11] To facilitate this comparison we have convoluted our results, assuming a triangular apparatus function of half-width 0.04 eV (corresponding to $\frac{3}{2}kT$ at room temperature and the approximate resolution of the Auerbach experiment). The results are shown in Fig. 3.

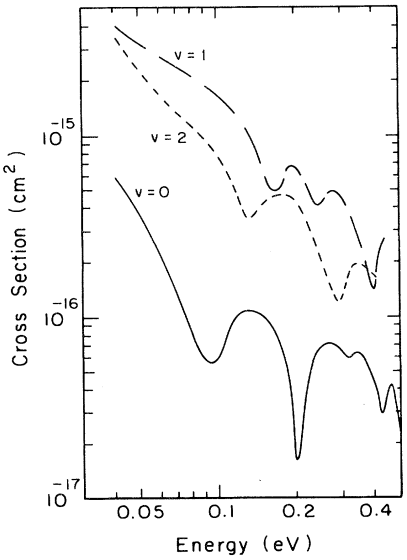

FIG. 3. Cross sections for e-H_2^+ recombination calculated by the MQDT approach and convoluted using a triangular apparatus function with a width of 0.04 eV (full width at half maximum): solid curve, $v_i=0$; long dashes, $v_i=1$; short dashes, $v_i=2$.

A second difficulty in comparing theory with experiment arises from the uncertainty concerning the vibrational state of the recombining ions in merged-beam experiments. Assuming that Auerbach *et al.* were successful in quenching states with $v \geq 3$, and that the populations of the lower states were proportional to the Franck-Condon factors governing transitions from neutral H_2, the relative populations would be approximately 20% ($v=0$), 40% ($v=1$), and 40% ($v=2$).[28] In Fig. 4 we compare the calculated cross sections, averaged in this manner, with the experimental results. Although there is qualitative agreement in regard to the magnitude of the cross section, the general energy dependence and the existence of window resonances, the calculated cross sections are smaller than the measured values, and there is little correlation in the position of the dips.

Comparison of Figs. 3 and 4 shows that the structures in the measured cross section correlate well with those in the calculated cross section for ground-state ions. This might suggest that the ions studied by Auerbach *et al.* are predominantly in the ground state. However, there would then be a major discrepancy in the magnitude of the cross section. The cross sections computed by Bottcher[5] for ground-state ions are also considerably smaller than the experimental values shown in Fig. 4.

Cross sections for dissociative recombination of electrons with H_2^+ ions have also been measured by Peart and Dolder[29] with the use of inclined beams. They obtained a value of 2.2×10^{-15} cm^2 at 0.33 eV, which is approximately twice the value measured by Auerbach *et al.*[11] They suggest that a significant fraction of the ions are in highly excited vibrational levels. Assuming that the level populations are determined by the Franck-Condon factors for ionization, Bottcher computed a value of $\sim1.7\times10^{-15}$ cm^2, in good agreement with experiment. Our estimate of the contribution from the $1\sigma_u^2\,{}^1\Sigma_g$ state is significantly lower. However, we believe that the higher resonant states make significant contributions to recombination to vibrationally excited ions, as discussed by Zhdanov and Chibisov.[30] Until the magnitude of these contributions is known, it seems inappropriate to compare our results with those of Peart and Dolder.[29]

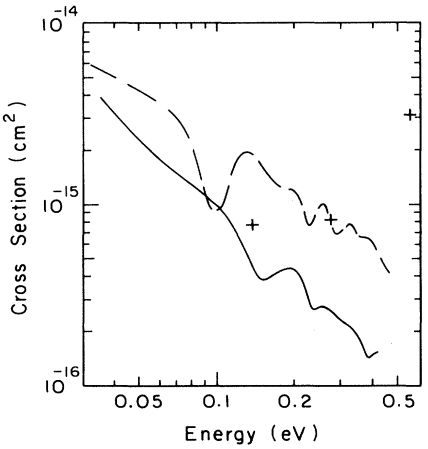

FIG. 4. Cross section for e-H_2^+ recombination with a mixture of ions in the $v=0,1,2$ states: solid curve, MQDT calculations; dashed curve, experiment (Ref. 11); crosses, calculations of Bottcher (Ref. 5). In both calculations the populations ratios have been taken as 1:2:2 for $v_i=0,1,2$, respectively.

B. Recombination rates

For most applications, one needs to know the rate of recombination for a swarm of electrons of varying energy. In particular, there is significant astrophysical interest in the recombination rates at low temperatures.

If direct recombination is dominant in the thermal regime, the calculation of the recombination rate would be straightforward, since the cross sections are inversely proportional to the energy of the incident electron. However, our 11-channel MQDT calculations for ground-state ions reveal the existence of a window resonance, due to the $v=7$ level of the $1s\sigma3d\sigma$ Rydberg state, at an energy of 5 meV. The presence of this resonance might reduce significantly the recombination rate at temperatures below 100 K. In order to check this result we performed a calculation using the CI approach with this single Rydberg state interacting with the electron scattering continuum. The window resonance appears in the cross section but it is shifted upwards by ~50 meV. The large magnitude of this shift, resulting from configuration interaction with the repulsive $1\sigma_u^2$ configuration, is due to the relatively low value of n^* for this state which leads to a large value for ρ_p^2 in Eq. (22). Indeed, the coupling between the Rydberg and non-Rydberg states is so strong that we should question whether our diabatic approach will lead to accurate predictions of the energy levels for such states. The alternative adiabatic approach has been used by Wolniewicz and Dressler[31] who predict that this state should lie 43 meV above the ground state of H_2^+, in good agreement with our CI analysis.

Using the cross sections computed by the CI method, the recombination rate for ground-state ions, at temperatures below 100 K, can be well represented by

$$\alpha_0(T)=1.7\times10^{-8}\left[\frac{100}{T}\right]^{0.5} \tag{46}$$

given in units of cm^{3}s^{-1}. Note that this value is very small compared with that found for most other molecules at similar temperature. For ions in the $v=1$ or 2 levels, the rate is given approximately by

$$\alpha_1(T)\approx1\times10^{-7}\left[\frac{100}{T}\right]^{0.5} \tag{47}$$

given in units of cm^{3}s^{-1}.

C. Resonant contributions to vibrational excitation

It is well established that shape resonances are important in the vibrational excitation of many neutral molecules by low-energy electrons. Resonances also occur in electron scattering by most molecular ions, but these resonances are usually Feshbach (core-excited) resonances. It might be helpful, therefore, for us to estimate the relative magnitudes of the resonant and nonresonant contributions to vibrational excitation in e-H_2^+ collisions.

The application of the MQDT to vibrational excitation

has already been described by Giusti, and the cross sections can be obtained from the S-matrix elements given in Eq. (23a) of Ref. 16. With the use of the CI approach of Sec. II, the cross section for vibrational excitation can be obtained directly from the amplitude $b_v(E)$ in the final channel. With the assumptions described following Eq. (14), we find

$$\sigma(v_i \to v_f) = \frac{\pi}{\epsilon}\omega \left| d_{v_f} + \sum_{p,v} \rho_p W_{v_f v} a_{pv} \right|^2 . \tag{48}$$

This result shows clearly that the doubly excited electronic state and the Rydberg states act as intermediate states in vibrational excitation. As in recombination, we expect to see narrow structures due to the Rydberg states superimposed upon, and interfering with, a smooth cross section due to the doubly excited state.

We have performed some preliminary calculations, without any closed channels, by both methods. Such calculations do not include Rydberg-state effects and show only the contribution from the $1\sigma_u^2\ {}^1\Sigma_g$ resonance. For $\sigma(0\to1)$ at 0.5 eV, the cross section is approximately 3×10^{-17} cm^2. Robb and Collins[32] have calculated vibrational excitation cross sections in the static exchange approximation, and find the total cross section for $\sigma(0\to1)$ to be $\sim7.5\times10^{-17}$ cm^2 at 0.54 eV. Thus the resonant contibution is small but not negligible. It seems probable that for transition to high vibrational levels ($v\geq2$) the cross sections will be dominated by this resonance. For example, we find $\sigma(0\to8)$ to be $\sim2\times10^{-18}$ cm^2 near threshold. Unfortunately, Robb and Collins[32] do not give results for such transitions.

The effects of the Rydberg states have been explored using the MQDT approach. The narrow structures resulting from the Rydberg levels are again mostly dips which lead to a significant reduction in the excitation cross section. Thus it appears that both the Rydberg states and the doubly excited electronic configurations should be included in accurate calculations of vibrational excitation in electron-ion collisions.

V. SUMMARY AND CONCLUSIONS

We have shown that unified theories of dissociative recombination, which take into account the formation of doubly excited electronic states and excited vibrational levels of Rydberg states, can be developed using either the configuration-interaction approach or MQDT. The latter approach is more suitable when many Rydberg series are included in the calculation, but the configuration-interaction method avoids the linearization of the K matrix describing the short-range interactions, which is a feature of current MQDT applications. This linearization leads to slight shifts in the positions of the structures associated with the Rydberg states, but does not lead to significant differences in the magnitude of the recombination rate.

The computed cross sections for e-H_2^+ recombination are in reasonable agreement with experiment in regard to the absolute magnitude of the cross section, the overall energy dependence and the appearance of the structures, which lead to narrow dips. In these respects, the results are significantly better than those of the last comprehensive theoretical study.[5] However, a quantitative comparison between theory and experiment will not be possible until measurements can be performed for ions in a single vibrational state.

For ground-state ions, the recombination rate is significantly smaller than that of many other diatomic molecules. Nevertheless, the rate is not sufficiently small that the process can be neglected in studies of the cooling of the primordial plasma in the early development of the universe. The recombination rates for low-lying excited vibrational states of the H_2^+ ion are larger than those for

TABLE I. Comparison of the symbols used in this work with those of Bardsley, Giusti, and Nitzan.

This work	Equation	Bardsley References 14 and 33	Giusti Reference 16	Nitzan Reference 23
$\chi_v(R)$	(4)[a]	$\zeta_d(R)$	$\chi^+_{v_0}(R)$	
$\chi_v(R)$	(4)[b]	$u_{1\nu}(R)$	$\chi_v(R)$	
$\phi_d(q,R)$	(4)	$\phi_d(q,R)$	$\Phi_{d_i}(q,r)$	
$\zeta_d(R)$	(4)	$\xi_d(R)$		
$V_{\rm el}(E,R)$	(7)	$V_{\alpha E}(R)$	$V^{\rm el}_{i,l}(\epsilon,R)$	
ρ_p	(9)	$(n^*)^{-1.5}$	$(n^*)^{-1.5}$	1
$W_{vv'}$	(11)	$V_{10}(E')$	$\xi_{\rm vib}/\pi$	$\rho_l^{1/2}V_{sl}$
$g_{vv'}$	(19)[c]	$V_\tau(R_0)g_{\tau\tau'}V_{\tau'}(R_0)$	$-i\xi_v\xi_{v'}/\pi$	
β	(21)		$(1+\xi^2_{v_0^+})^{-1}$	$(1+N)^{-1}$
$F_{1E}(R)$	(23)	$u_{\rm I}(R)$	$F_{d_i}(K,R)$	
$F_{2E}(R)$	(24)[d]	$u_{\rm II}(R)$	$i[F_{d_i}(K,R)+iG_{d_i}(K,R)]$	
$V_v(E)$	(25)		ξ_v/π	$\rho_m^{1/2}V_{sm}$
$V_{v_i}(E)$	(25)		$\xi^+_{v_0}/\pi$	$\rho_l^{1/2}\rho_m^{1/2}V_{lm}$
$\sigma_{\rm DR}(E)$	(30)	$\sigma(E)$	$\sigma^+_{dv_0}$	$\sigma_{\rm NR}$

[a]Vibrational wave function for the molecular ion.
[b]Vibrational wave function for the neutral Rydberg state, which in this work is assumed to be the same as that of the ion.
[c]This matrix element contains a real part which is neglected in Ref. 16.
[d]These outgoing nuclear wave functions are normalized in different ways.

the ground state.

Our brief examination of the effects of the same intermediate states upon vibrational excitation in e-H_2^+ collisions suggests that their effects should be taken into account for transitions with $\Delta v \geq 2$. Further studies of vibrational excitation in electron-ion collisions via the MQDT approach would be worthwhile.

It seems possible that the best features of these two methods could be combined through an improved calculation of the short-range K matrix that appears in the MQDT theory. The Green-function techniques of Sec. II could be used in the evaluation of K, and the connection between the CI wave function, used solely in the core region, and the scattering matrix elements, that determine the cross sections, should be obtained through the MQDT formalism.

We have confined our attention to recombination through the lowest doubly excited state of H_2. For electrons with energy greater than 2 eV, or for ions in more highly excited vibrational states, the contributions of other doubly excited states become more important. The $^3\Sigma$ and $^3\Pi$ states are of special interest because of their larger statistical weights. More information on the potential curves and autoionization widths is required before their contributions can be assessed.

ACKNOWLEDGMENTS

We are indebted to Ch. Jungen and M. Roult for permitting us to use their MQDT subroutine, to H. Lefebvre-Brion for numerous fruitful discussions, and to A. Hazi for supplying the results of his calculations in advance of publication. Part of this work was supported by the National Science Foundation, Theoretical Physics Program, through Grant No. PHY-81-05074.

APPENDIX: COMPARISON OF NOTATION

One of the major goals of this work was to bring together two apparently disparate approaches to the same problem. In doing this we have chosen our notation to simplify the comparison with both sets of earlier papers. This notation does not correspond exactly to that used previously by Bardsley[14,33] or Giusti.[16] Table I gives the correspondence in the notations of these papers.

We have noted the analogy between this treatment of dissociative recombination and Nitzan's study of atomic resonances in photon absorption and electron-ion scattering. Where there is a direct correspondence between quantities in this work and those in Nitzan's paper,[24] this is also indicated in the table. However, it must be stressed that this correspondence is an analogy between symbols with different physical meanings.

[1]J. N. Bardsley and M. A. Biondi, Adv. At. Mol. Phys. 6, 1 (1970).
[2]J. B. A. Mitchell and J. W. McGowan, in *Physics of Electron-Ion and Ion-Ion Collisions,* edited by Brouillard (Plenum, New York, 1982).
[3]F. L. Walls and G. H. Dunn, J. Geophys. Res. 79, 1911 (1974).
[4]R. A. Heppner, F. L. Walls, W. T. Armstrong, and G. H. Dunn, Phys. Rev. A 13, 1000 (1976).
[5]C. Bottcher, J. Phys. B 9, 2899 (1976).
[6]A. U. Hazi, C. Derkits, and J. N. Bardsley, Phys. Rev. A 27, 1751 (1983).
[7]H. Takagi and H. Nakamura, in *Abstracts of the XII International Conference on the Physics of Electronic and Atomic Collisions, Gatlinburg, Tennessee, 1981,* edited by S. Datz (North-Holland, Amsterdam, 1981), p. 457.
[8]D. W. Robb (private communication).
[9]B. Peart and K. T. Dolder, J. Phys. B 7, 236 (1974).
[10]D. Mathur, S. U. Khan, and J. B. Hasted, J. Phys. B 11, 3615 (1978).
[11]D. Auerbach, R. Cacak, R. Caudano, T. D. Gaily, C. J. Keyser, J. W. McGowan, J. B. A. Mitchell, and S. F. J. Wilk, J. Phys. B 10, 3797 (1977).
[12]D. R. Bates, Phys. Rev. 78, 492 (1950).
[13]U. Fano, Phys. Rev. 124, 1866 (1961).
[14]J. N. Bardsley, J. Phys. B 1, 349 (1968).
[15]C. Bottcher, Proc. R. Soc. London Ser. A 340, 301 (1974).
[16]A. Giusti, J. Phys. B 13, 3867 (1980).
[17]T. F. O'Malley, J. Phys. B 14, 1229 (1981).
[18]C. M. Lee, Phys. Rev. A 16, 109 (1977).
[19]A. Dalgarno, in Ref. 2.
[20]R. S. Berry, J. Chem. Phys. 45, 1228 (1966).
[21]J. N. Bardsley, Chem. Phys. Lett. 1, 229 (1967).
[22]G. Herzberg and C. Jungen, J. Mol. Spectrosc. 41, 425 (1972).
[23]U. Fano and F. Prats, J. Natl. Acad. Sci. India, A 33, 553 (1963).
[24]A. Nitzan, Mol. Phys. 27, 65 (1974).
[25]R. Lefebvre and J. A. Beswick, Mol. Phys. 23, 1223 (1972); J. A. Beswick and R. Lefebvre, *ibid.* 29, 1611 (1975).
[26]C. Jungen and O. Atabek, J. Chem. Phys. 66, 5584 (1977).
[27]C. Jungen and D. Dill, J. Chem. Phys. 73, 3338 (1980).
[28]F. Von Busch and G. H. Dunn, Phys. Rev. A 5, 1725 (1972).
[29]B. Peart and K. T. Dolder, J. Phys. B 7, 236 (1974).
[30]V. P. Zhdanov and M. I. Chibisov, Zh. Eksp. Teor. Fiz. 74, 75 (1978) [Sov. Phys.—JETP 47, 38 (1978)].
[31]L. Wolniewicz and K. Dressler, J. Mol. Spectrosc. 77, 286 (1979).
[32]W. D. Robb and L. A. Collins, Phys. Rev. A 22, 2474 (1980).
[33]J. N. Bardsley, J. Phys. B 1, 365 (1968).